Nyquist Plots Prediction Using Neural Networks in Corrosion Inhibition of Steel by Schiff Base

Akbarzade, Kazem; Danaee, Iman*+

Abadan Faculty of Petroleum Engineering, Petroleum University of Technology, Abadan, I.R. IRAN

ABSTRACT: *The corrosion inhibition effect of N,N'-bis(n-Hydroxybenzaldehyde)-1,3-Propandiimine on mild steel has been investigated in 1 M HCl using electrochemical impedance spectroscopy. A predictive model was presented for Nyquist plots using an artificial neural network. The proposed model predicted the imaginary impedance based on the real part of the impedance as a function of time. The model took into account the variations of the real impedance and immersion time of steel in a corrosive environment, considering constant corrosion inhibitor concentrations. The best-fit training data set was obtained with eleven neurons in the hidden layer for Schiff base inhibitor, which made it possible to predict the efficiency. On the validation data set, simulations and experimental data test were in good agreement. The developed model can be used for the prediction of the real and imaginary parts of the impedance as a function of time.*

KEYWORDS: *Impedance; Neural network; Corrosion; Inhibitor.*

INTRODUCTION

Acid solutions with pH values below one are generally used for industrial acid cleaning, acid descaling, oil well acidizing, the pickling and removal of undesirable rust [1]. Mild steel which is extensively used in a lot of industrial processes could corrode during these acidic applications particularly with the use of HCl [2,3].

The use of inhibitors is one of the most practical methods for protection against corrosion, especially in acidic media. Many studies have been made on the corrosion and inhibition of steels in acidic solution [4-6]. Among numerous inhibitors that have been tested and applied industrially, those that are nontoxic or of low toxicity, are now far more strategic than in the recent past. Organic compounds bearing heteroatoms with high electron density such as phosphor, sulfur, nitrogen, oxygen or those containing multiple bonds which are considered as adsorption centers, are effective as corrosion inhibitors [7-10].

Schiff base, the condensation product of aldehydes or ketones with amines is shown to have effective corrosion inhibitions for different metals and alloys in acidic media [11]. The efficiency of the Schiff base is much higher than that of the corresponding aldehyde and amines, and this may be due to the presence of a -C=N-group in the molecules [12,13].

Different experimental electrochemical techniques are used to study the corrosion inhibition behavior of inhibitors in different environments [14]. Impedance spectroscopy is an electrochemical technique used in corrosion studies. This method uses an alternating current (AC) that is applied over an electrode to obtain the corresponding response. Electrochemical impedance

can be extended by using Artificial Neural Network (ANN) [15-17]. ANNs are computational systems that correlate a pattern between groups of input observations (real data) and a group of output observations (results). ANN can be used to predict different impedance Nyquist plots from different inhibitor concentrations without experimentation in the time domain [15-17].

Neural networks are parallel-distributed information processing systems used for empirical regression and classification modeling [18-22]. A neural network is trained on a set of examples of input and output data. The outcome of this training is a set of coefficients (called weights) and a specification of the functions which is in combination with the weights relate the input to the output. Once the network is trained, the estimation of the outputs for any given inputs is very rapid [23,24]. Artificial Neural Network (ANN) consists of artificial neurons grouped into layers that are put in relation to each other by parallel connections [25]. For every ANN, the first layer constitutes the input layer (input variables) and the last one forms the output layer (output variables). Between them, one or more neuron layers called hidden layers may be located. The most widely used transfer function for the input and a hidden layer is the sigmoid transfer function which may be expressed as:

$$f(x) = \frac{1}{1 + \exp(-x)} \tag{1}$$

The sigmoid transfer function takes the input, which can have any value between plus and minus infinity, and squashes the output into the range -1 to 1. The linear transfer function used as the output layer transfer function [26]:

$$f(x) = x \tag{2}$$

The standard network structure for an approximation function is the feedforward network. The feedforward network often has one or more hidden layers of sigmoid neurons followed by an output layer of linear neurons [27]. Multiple layers of neurons with nonlinear transfer functions allow the network to learn nonlinear and linear relationships between input and output vectors. The linear output layer lets the network produce values outside the −1 to +1 range [28]. For the network, the appropriate notation is used in two-layer networks [29]. The associated coefficients with the hidden layer are grouped into matrices W_i (weights) and b_1 (biases) as well as

the associated coefficients with the output layer are grouped into matrices W_o and b_2. The number of neurons in the input and output layers is given, respectively, by the number of input and output variables in the process under investigation. The optimal number of neurons in the hidden layer(s) is difficult to specify and depends on the type and complexity of the process, or experimentation. This number is usually iteratively determined.

The purpose of the present study is to investigate the inhibition effect of synthesized Schiff base N,N′-bis(3-Hydroxybenzaldehyde)-1,3-Propandiimine on corrosion of mild steel in 1 M HCl. The experimental method of Electrochemical Impedance Spectroscopy (EIS) was used to study the inhibition effect. Artificial neural network model was applied to predict different impedance Nyquist plots without experimental variations in the time domain. Neural network model was developed and trained with experimental data from impedance to know the performance of corrosion inhibitor. The obtained results by the neural network model were compared with tested experimental data.

EXPERIMENTAL SECTION

All chemicals used in present work were of reagent-grade Merck product and used as received without further purification. Schiff base was prepared according to the described procedure [13,30]. To a stirred ethanolic solution (20 mL) of 1,3-diaminopropane (0.074 g, 1 mmol), 3-hydroxybenzaldehyde (0.122 g, 2 mmol) was added. The light yellow to the light brown solution was stirred and heated to reflux for 6 h. A light yellow to light brown precipitate was obtained that was filtered off and washed with diethyl ether, Yield (98%). Analysis calculated for $C_{17}H_{18}N_2O_2$ (282.3): C, 72.32; H, 6.42; N, 9.92. Found: C, 72.75; H, 6.01; N, 9.99%. Identification of the structure of the synthesized Schiff base was performed by IR, ^{1}HNMR and ^{13}C-NMR spectroscopic techniques. The Schiff base used in this study is presented in Fig. 1.

Working electrodes were prepared from Mild steel specimens with chemical composition (wt.%) C=0.16%, Si=0.32%, Mn=0.35%, P=0.03%, S=0.02%, and the remainder Fe. Samples were cut from a cylindrical rod with a cutter machine. The exposed surface area of each electrode is equal to 0.81 cm[2]. These specimens were used as the working electrode in electrochemical measurements and the exposed areas of the electrodes were mechanically
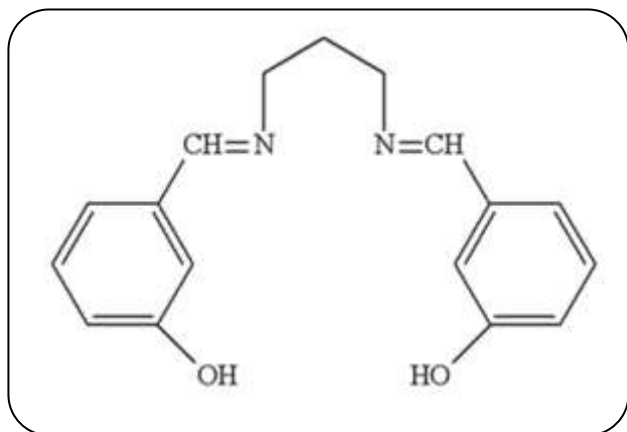
       Research Article

Fig. 1: The chemical structure of the Schiff base, N,N'-bis(3-Hydroxybenzaldehyde)-1,3-Propandiimine.

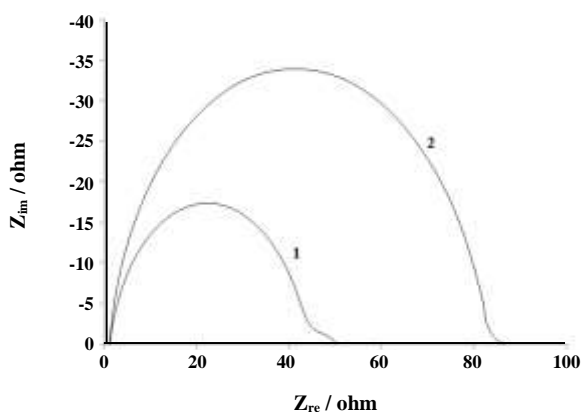***Fig. 2: Nyquist plots for mild steel in 1 M HCl (1) without and (2) with 2×10⁻⁴ M inhibitor.***

abraded with 220, 400, 600, 800, 1000 and 1200 grades of emery paper, degreased with acetone and rinsed by distilled water before each electrochemical experiment.

Electrochemical measurements were carried out in a conventional three-electrode system. A Saturated Calomel Electrode (SCE) was used as the reference electrode and a platinum sheet was used as the counter electrode. Before each experiment, the working electrode was immersed in the test cell for 30 min until to reach steady state condition. The electrochemical measurements were carried out using computer controlled Auto Lab potentiostat/galvanostat (PGSTAT 302N). All tests were carried out at constant temperatures by controlling the cell temperature using a water bath. All the experiments were performed in quiescent conditions and the solutions were open to the atmosphere under unstirred conditions.

Electrochemical Impedance Spectroscopy (EIS) measurements were carried out in the frequency range of 100 kHz to 10 MHz with an amplitude of 10 mV peak-to-peak using AC signals at open circuit potential. Fitting of experimental impedance spectroscopy data to the proposed equivalent circuit was done by means of home written least square software based on the Marquardt method for the optimization of functions and Macdonald weighting for the real and imaginary parts of the impedance [31,32].

RESULTS AND DISCUSSION
Electrochemical impedance spectroscopy

Fig. 2 shows Nyquist plots recorded for the corrosion of steel in 1 M HCl solution in the absence and presence of inhibitor obtained at E_{corr}. The plots indicate a depressed capacitive loop which arises from the time constant of the electrical double layer and charge transfer resistance. The impedance of the inhibited steel increases in the presence of inhibitor and consequently results the inhibition behavior of this compound. The equivalent circuit compatible with the Nyquist diagram recorded with and without inhibitor was depicted in Fig. 3.

The simplest approach requires the theoretical transfer function $Z(\omega)$ to be represented by a parallel combination of a resistance R_{ct} and a capacitance C, both in series with another resistance R_s [33]:

$$Z(\omega) = R_s + \frac{1}{1/R_{ct} + i\omega C} \tag{3}$$

ω is the angular frequency in rad/s, $\omega = 2\pi f$, and f is the frequency in Hz.

To obtain a satisfactory impedance simulation of steel, it is necessary to replace the capacitor (C) with a constant phase element (CPE) Q in the equivalent circuit. The most widely accepted explanation for the presence of CPE behavior and depressed semicircles on solid electrodes is microscopic roughness, causing an inhomogeneous distribution in the solution resistance as well as in the double-layer capacitance [34]. Constant phase element CPE_{dl}, R_s and R_{ct} can correspond to double layer capacitance, solvent resistance, and charge transfer resistance respectively. To corroborate the equivalent circuit, the experimental data are fitted to the equivalent circuit and the circuit elements are obtained. Table 1 illustrates the equivalent circuit parameters

Table 1: Impedance data for steel in 1 M HCl solution without and with inhibitor.

Concentration/M	R_s/ Ω	R_{ct}/ Ω	$Q_{dl} \times 10^3$/ F	n
Blank	1.5	42	2.5	0.86
2.0×10^{-4}	1.4	81	0.5	0.92
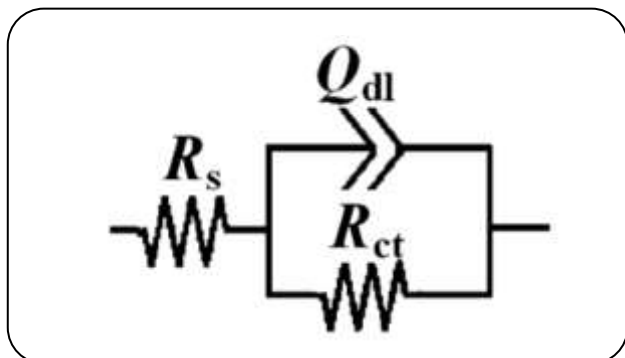
Fig. 3: Equivalent circuits compatible with the experimental impedance data in Fig. 2 for corrosion of steel electrode without and with inhibitor.

for the impedance spectra of corrosion of steel in 1 M HCl solution.

The results demonstrate that in the presence of 2×10^{-4} M inhibitor, the double layer capacitance decreases and the charge transfer resistance enhances. The decrease in Q_{dl} values is caused by adsorption of inhibitor indicating that the exposed area decreases. On the other hand, a decrease in Q_{dl}, which can result from a decrease in local dielectric constant and/or an increase in the thickness of the electrical double layer, suggests that Schiff base inhibitor acts by adsorption at the metal–solution interface.

As the Q_{dl} exponent (*n*) is a measure of the surface heterogeneity, values of *n* indicate that the steel surface becomes more homogeneous in the presence of inhibitor as a result of its adsorption on the steel surface and corrosion inhibition [35].

The effect of immersion time was determined by exposing the mild steel in 1 M HCl solution containing an inhibitor. Electrochemical impedance method is a useful technique for long time tests; because it does not disturb the system significantly and it is possible to follow it overtime. Therefore, the results were followed by EIS, and impedance spectra were measured in different exposure times. Time dependency of mild steel in 1 M HCl solution in the presence of 2×10^{-4} M of inhibitor are presented in Fig. 4 and the corresponding impedance

parameters are indicated in Table 2. The inhibition efficiency of studied Schiff base increases with increasing immersion time from 30 min to 24 hr. This increase in *IE%* is probably due to the more complete and stable surface coverage of the electrode with inhibitor molecules and an improvement in the quality of the protective film with time. In addition, the double layer capacitance decreases with increasing immersion time due to the completion of the inhibitor layer. In higher immersion time the charge transfer resistance decreases which is due to the deterioration of the inhibitor layer.

Neural network

The obtained experimental database was split into three parts: a training set containing 70% of the data (350 random observations), a validation set containing 10% of the data (50 random observations) and testing set containing 20% of the data (100 observations). The experimental data from the Nyquist plot obtained in the presence of inhibitor during 30 min, 1, 4, 8, 12, 16, 20, 24, 26 and 30 h immersion were used for training the neural network model. Number of input data used in the network is 500.

For the purpose of this work a feedforward network consisting of two layers was tested: a hidden layer with 11 neurons and an output linear layer with 1 neuron to determine the imaginary impedance evolution for different immersion times in a constant inhibitor concentration (Fig. 5). The transfer function used in the hidden layer is hyperbolic tangent sigmoid transfer function (tan sig):

$$\tan \text{sig}(n) = 1 - \frac{2}{1 + e^{-2n}} \tag{4}$$

The input layers for these neural network models were real impedance and time (in hours). All calculations were carried out with MATLAB software version 7.12.0.635 (R2011a) and Neural Network Toolbox version 7. In order to determine the optimal number of hidden layer nodes, neural networks with different

Research Article

Table 2: Impedance data for steel in different immersion time in 1 M HCl solution in the presence of inhibitor.

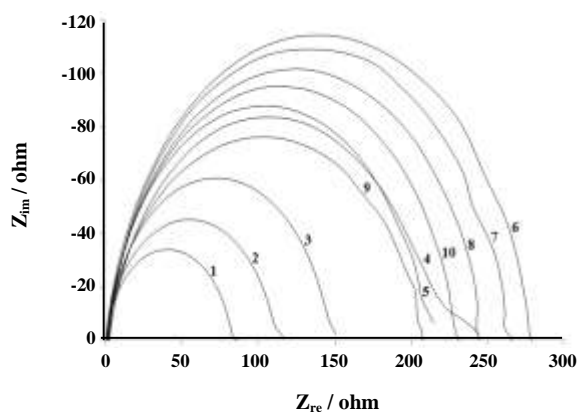| Concentration/M	R_s/ Ω	R_{ct}/ Ω	$Q_{dl}\times10^3/ F$	n
30 min	1.4	81	0.5	0.92
1 h	1.4	107	0.4	0.91
4 h	1.3	145	0.4	0.91
8 h	1.3	205	0.3	0.90
12 h	1.4	206	0.4	0.88
16 h	1.2	275	0.2	0.93
20 h	1.2	253	0.3	0.91
24 h	1.3	241	0.3	0.91
26 h	1.2	202	0.6	0.88
30 h	1.2	227	0.5	0.89

Fig. 4: The effect of immersion time on mild steel in 1 M HCl in the presence of 2×10^{-4} M inhibitor: (1) 30 min, (2) 1h, (3) 4 h, (4) 8 h, (5) 12 h, (6) 16 h, (7) 20 h, (8) 24 h, (9) 26 h and (10) 30 h.
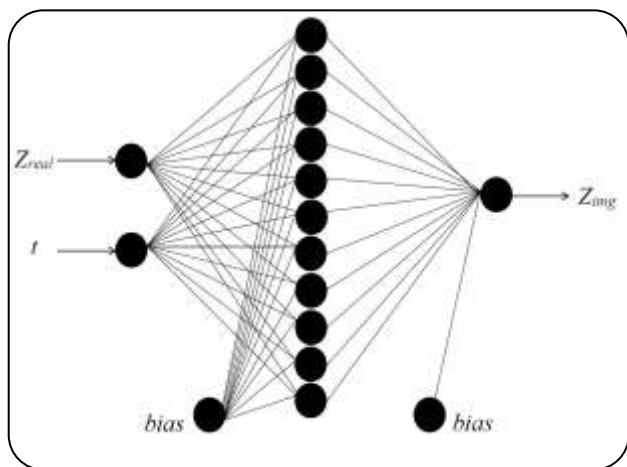

Fig. 5: Neural architecture.

a number of hidden layer nodes were trained. For the experimental data used to train the network, the optimum number of hidden layer nodes was chosen when the error was minimum by varying the learning rate and momentum. For selecting the number of neurons in the hidden layers, it is necessary to consider that if too few neurons are used, the ANN is not capable of fitting an input-output mapping, but if too many neurons are used overfitting can happen [36]. The performance of the model at different hidden neuron levels is shown in Fig. 6. The number of evaluated neurons range from 1 to 12. Neurons more than 12 were not tried in order to avoid over-fitting [37]. It can be observed that the ANN model with 11 hidden neurons produce the best performance and is considered to be the optimal configuration for the present problem. According to the obtained model, Table 3 gives the optimum coefficients (Wi, Wo, B1, and B2) of the best fit of the model for nine neurons in the hidden layer.

The predictability of the developed model is quantified in terms of the correlation coefficient (R). These are defined below:

$$R = \frac{\sum_{i=1}^{N}\left(E_i - \overline{E}\right)\left(P_i - \overline{P}\right)}{\sqrt{\sum_{i=1}^{N}\left(E_i - \overline{E}\right)^2 \sum_{i=1}^{N}\left(P_i - \overline{P}\right)^2}} \tag{5}$$

Where *E* is the experimental finding and *P* is the predicted value obtained from the neural network model. $\overline{E}$ and $\overline{P}$ are the mean values of *E* and *P* respectively [37]. A good model would have most of the points close to the diagonal line [38]. Fig. 7 presents the simulated

Table 3: Adjusted parameters for the best neural network.

Wi$_1$	
-0.281	5.557
-0.334	10.851
0.334	-1.785
-0.811	0.777
-1.268	-5.869
5.712	36.610
0.032	2.419
0.136	1.792
0.832	-7.767
-5.629	0.072
1.039	-10.808

Wo$_2$									
-30.32	13.7	-28.79	-15.43	-5.072	-0.386	16.35	-20.71	-21.75	20.46	19.54

b$_1$									
5.2113	9.965	-1.819	1.268	5.712	-5.289	-0.397	-0.151	7.361	-7.608	9.852

b$_2$
31.79694
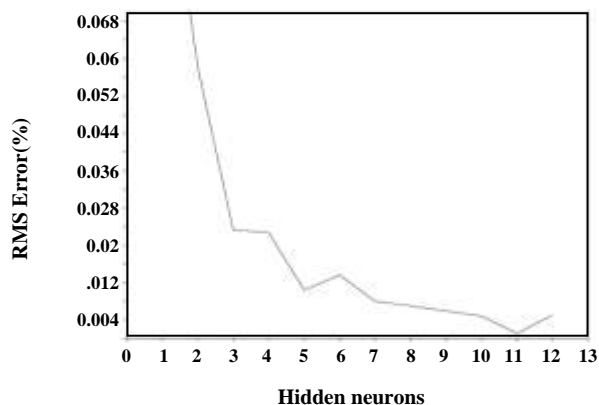
Fig. 6: Performances of the ANN model at various hidden neurons level.

Fig. 7: Comparison of simulated and experimental Z values.

imaginary impedance against the experimental imaginary impedance database for all Nyquist plots. It can be observed that a very good correlation between experimental and predicted data is obtained. No scattering in the data points can be observed throughout the data range. The correlation factor for the present model is R^2=0.9952 indicating that the fit has a very high
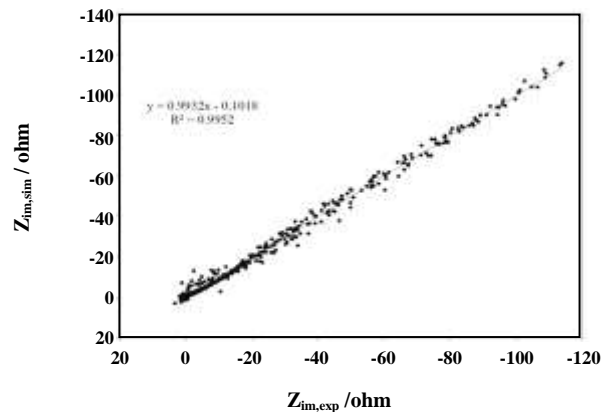
degree of accuracy. The distribution between predicted values and the experimental values are modeled using linear approaches and a best linear equation is obtained. The equation is also given in Fig. 7.

According to these results, the developed model is able to predict the imaginary impedance as a function of input parameters throughout the experimental domain.
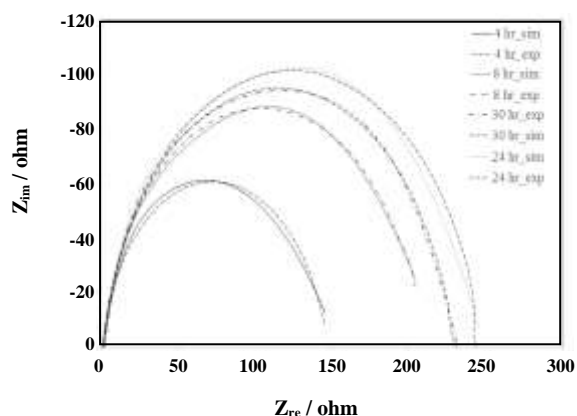
Research Article

Fig. 8: Comparison of experimental and simulated Nyquist plots.

Fig. 8 depicts the ability of the model to predict the impedance value as a function of time for 2×10^{-4} M of inhibitor. As can be seen, the simulated Nyquist diagrams are in good agreement with the experimental data. These models are important to determine the corrosion resistance over this experimental condition. The results obtained by the above analysis lead to the conclusion that the models are successful in predicting the impedance value as a function of time. This model is not too complex because the simulation is performed by simple arithmetic operations and, therefore, it can be used to predict Nyquist plots over different immersion times and to determine different impedance behavior with confidence.

CONCLUSIONS

This work showed that the neural network could be used in the electrochemical impedance techniques. The results of this study were:

• ANN-based model was developed to simulate the imaginary impedance in the Nyquist plots and used a feed-forward network and an algorithm Levenberg-Marquardt backpropagation modification to training the neural network.

• The developed model could predict the Nyquist plot and the predicted response of this model was in very good agreement with experimental data.

• This model was not complex because the simulation was achieved via simple arithmetic operations, and therefore it could be used for the estimation of the electrochemical impedance over a wide range of experimental conditions.

• One of the highlights of this model was that it could spread without any preliminary assumptions on the underlying corrosion or chemical mechanisms.

REFERENCES

[1] Hegazy M.A., Aiad I., 1-Dodecyl-4-(((3-Morpholinopropyl)imino)methyl)pyridin -1- Ium Bromide as a Novel Corrosion Inhibitor for Carbon Steel During Phosphoric Acid Production, *J. Ind. Eng. Chem.* **31**: 91-99 (2015).

[2] Shabani-Nooshabadi M., Ghandchi M.S., Santolina Chamaecyparissus Extract as a Natural Source Inhibitor for 304 Stainless Steel Corrosion in 3.5% NaCl, *J. Ind. Eng. Chem.* **31**: 231-237 (2015).

[3] Hoseinzadeh A.R., Danaee I., Maddahy, M.H., RashvandAvei, M., Taurine as a Green Corrosion Inhibitor for AISI 4130 Steel Alloy in Hydrochloric Acid Solution. *Chem. Eng. Comm.*, **201**: 380-402 (2014).

[4] ChaitraT.K., Mohana K.N.S., Tandon H.C., Thermodynamic, Electrochemical and Quantum Chemical Evaluation of Some Triazole Schiff Bases as Mild Steel Corrosion Inhibitors in Acid Media, *J. Mol. Liq.*, **211**: 1026-1038 (2015).

[5] Verma C., Ebenso E.E., Bahadur I., Obot I.B., Quraishi M.A., 5-(Phenylthio)-3H-pyrrole-4-Carbonitriles as Effective Corrosion Inhibitors for Mild Steel in 1 M HCl: Experimental and Theoretical Investigation, *J. Mol. Liq.*, **212**: 209-218 (2015).

[6] Park J.K., Jeong N.H., Corrosion Inhibition Effect of Ester Containing Cationic Gemini Surfactants on Low Carbon Steel, *Iran. J. Chem. Chem. Eng. (IJCCE),* **35**: 85-93 (2016).

[7] Abderrahim K., Abderrahmane S., Millet J.P., Inhibition of Copper Corrosion by Ethanolamine in 100 ppm NaCl, *Iran. J. Chem. Chem. Eng. (IJCCE)* **35**: 89-98 (2016).

[8] Gholami M., Danaee I., Maddahy M.H., RashvandAvei M., Correlated ab Initio and Electroanalytical Study on Inhibition Behavior of 2‑Mercaptobenzothiazole and Its Thiole−Thione Tautomerism Effect for the Corrosion of Steel (API 5L X52) in Sulphuric Acid Solution. *Ind. Eng. Chem. Res.* **52**: 14875−14889 (2013).

[9] Danaee I., Ghasemi O., Rashed G. R., RashvandAvei M., Maddahy M.H., Effect of Hydroxyl Group Position on Adsorption Behavior and Corrosion Inhibition of Hydroxybenzaldehyde Schiff Bases: Electrochemical and Quantum Calculations. *J. Mol. Struct.* **1035**, 247-259 (2013).

[10] Balaji J., Sethuraman M.G., Corrosion Protection of Copper with Hybrid Sol-Gel Containing 1H-1, 2, 4-triazole-3-thiol, *Iran. J. Chem. Chem. Eng. (IJCCE)* **35**: 61-71 (2016).

[11] Ghasemi O., Danaee I., Rashed G.R., RashvandAvei M., Maddahy M.H., Inhibition effect of a synthesized N, N′-bis(2-hydroxybenzaldehyde)-1, 3-propandiimine on Corrosion of Mild Steel in HCl. *J. Cent. South Univ.* **20**: 301-311 (2013).

[12] Dasami P.M., Parameswari K., Chitra S., Corrosion Inhibition of Mild Steel in 1 M H_2SO_4 by Thiadiazole Schiff Bases, *Measurement*, **69**: 195-201 (2015).

[13] Jafari H., Danaee I. Eskandari H., RashvandAvei M., Electrochemical and Theoretical Studies of Adsorption and Corrosion Inhibition of N,N′-Bis(2-hydroxyethoxyacetophenone) -2,2-dimethyl -1,2-propanediimine on Low Carbon Steel (API 5L Grade B) in Acidic Solution. *Ind. Eng. Chem. Res.*, **52**: 6617-6632 (2013).

[14] Saha S. K., Ghosh P., Hens A., Murmu N.C., Banerjee P., Density Functional Theory and Molecular Dynamics Simulation Study on Corrosion Inhibition Performance of Mild Steel by Mercapto-Quinoline Schiff Base Corrosion Inhibitor, *Physica E*, **66**: 332-341 (2015).

[15] Colorado-Garrido D., Serna S., Cruz-Chávez M., Hernández J.A., Campillo B., Artificial Neural Networks for Electrochemical Impedance Spectroscopy Sour Corrosion Predictions of Nano-modified Microalloyed Steels, *Electronics, Robotics and Automotive Mechanics Conference*, **210**: 185-190 (2010).

[16] Silva C.D.L.D., Junior G.C., Morais A.P.D., Marchesan G., Guarda F.G.K., A Continually Online Trained Impedance Estimation Algorithm for Transmission Line Distance Protection Tolerant to System Frequency Deviation, *Electr. Pow. Syst. Res.* **147**: 73-80 (2017).

[17] Conesa C., Sánchez L.G., Seguí L., Fito P., Laguarda-Miró N., Ethanol Quantification in Pineapple Waste by an Electrochemical Impedance Spectroscopy-Based System and Artificial Neural Networks, *Chemometr. Intell. Lab.* **161:** 1-7 (2017).

[18] Ghanadzadeh H., Daghbandan A., Akbarizadeh M., Applying Pareto Design of GMDH-Type Neural Network for Solid-Liquid Equilibrium of Binary Systems (Isotactic Poly 1-Butene (1)-Organic Solvents (2)), *Iran. J. Chem. Chem. Eng. (IJCCE)*, **33**: 67-73 (2014).

[19] Ehsani M.R., Bateni H., Razi Parchikolaei G., Modeling of Oxidative Coupling of Methane over Mn/Na2WO4/SiO2 Catalyst Using Artificial Neural Network, *Iran. J. Chem. Chem. Eng. (IJCCE),* **32**: 107-114 (2013).

[20] Ahmmed I.S., Mohamed H.A., Nayef G.M., Decentralized Advanced Model Predictive Controller of Fluidized-Bed for Polymerization Process, *Iran. J. Chem. Chem. Eng. (IJCCE),* **31**: 91-117 (2012).

[21] Azari A., Shariaty-Niassar M., Alborzi M., Short-term and Medium-term Gas Demand Load Forecasting by Neural Networks, *Iran. J. Chem. Chem. Eng. (IJCCE),* **31**: 77-84 (2012).

[22] Magharei A., Vahabzadeh F., Sohrabi M., Rahimi Kashkouli Y., Maleki M., Mixture of Xylose and Glucose Affects Xylitol Production by Pichia guilliermondii: Model Prediction Using Artificial Neural Network, *Iran. J. Chem. Chem. Eng. (IJCCE),* **31**: 119-131 (2012).

[23] Abbasi M., Soleymani A.R., Parssa J.B., Operation Simulation of a Recycled Electrochemical Ozone Generator Using Artificial Neural Network, *Chem. Eng. Res. Des.,* **92**: 2618-2625 (2014).

[24] Chen F.F., Breedon M., White P., Chu C., Mallick D., Thomas S., Sapper E., Cole I., Correlation between Molecular Features and Electrochemical Properties Using an Artificial Neural Network, *Mater. Des.* **112**: 410-418 (2016).

[25] Panchal I., Sawhney I.K., Sharma A.K., Dang A.K., Classification of Healthy and Mastitis Murrah Buffaloes by Application of Neural Network Models Using Yield and Milk Quality Parameters, *Comput. Electron. Agr.* **127**: 242-248 (2016).

[26] Rolich T., Rezic I., Curkovic L., Estimation of Steel Guitar Strings Corrosion by Artificial Neural Network, *Corros. Sci.* **52**: 996-1002 (2010).

[27] Sun Y., Chen Y., Yuan Y., Wang G., Dynamic Adjustment of Hidden Layer Structure for Convex Incremental Extreme Learning Machine, *Neurocomputing,* **261**: 83-93 (2017).

[28] Yang Z.X., Zhao G.H., Rong H.J., Yang J., Adaptive Backstepping Control for Magnetic Bearing System via Feedforward Networks with Random Hidden Nodes, *Neurocomputing* **174**: 109-120 (2016).

[29] Matias T., Souza F., Araújo R., Antunes C.H., Learning of a Single-Hidden Layer Feedforward Neural Network Using an Optimized Extreme Learning Machine, *Neurocomputing* **129**: 428-436 (2014).

[30] Jafari H., Danaee I., Eskandari H., RashvandAvei M., Combined Computational and Experimental Study on the Adsorption and Inhibition Effects of N_2O_2 Schiff Base on the Corrosion of API 5L Grade B Steel in 1 mol/L HCl, *J. Mater. Sci. Technol.*, **30**: 239-252 (2014).

[31] Danaee I., Kinetics and Mechanism of Palladium Electrodeposition on Graphite Electrode by Impedance and Noise Measurements, *J. Electroanal. Chem.*, **662**: 415–420 (2011).

[32] Macdonald J.R., Note on the Parameterization of the Constant Phase Admittance Element. *Solid State Ion.,* **13**: 147–149 (1984).

[33] Hoseinzadeh A.R., Danaee I., Maddahy M.H., Thermodynamic and Adsorption Behaviour of Vitamin B1 as a Corrosion Inhibitor for AISI 4130 Steel Alloy in HCl Solution, *Z. Phys. Chem.,* **227**: 403-417 (2013).

[34] RameshKumar S., Danaee I., RashvandAvei M., Vijayan M., Quantum Chemical and Experimental Investigations on Equipotent Effects of (+)R and (−)S Enantiomers of Racemic Amisulpride as Eco-Friendly Corrosion Inhibitors for Mild steel in Acidic Solution, *J. Mol. Liq.*, **212**: 168-186 (2015).

[35] Danaee I., Niknejad Khomami M., Attar A.A., Corrosion Behavior of AISI 4130 Steel Alloy in Ethylene Glycol–Water Mixture in Presence of Molybdate, *Mater. Chem. Phys.,* **135**: 658–667 (2012).

[36] Martin O., De Tiedra P., Lopez M., Artificial Neural Networks for Pitting Potential Prediction of Resistance Spot Welding Joints of AISI 304 Austenitic Stainless Steel, *Corros. Sci.* **52**: 2397-2402 (2010).

[37] Ramana K.V.S., Anita T., Mandal S., Kaliappan S., Shaikh H., Sivaprasad P.V., Dayal, R.K., Khatak H.S., Effect of Different Environmental Parameters on Pitting Behavior of AISI Type 316L Stainless Steel: Experimental Studies and Neural Network Modeling, *Mater. Des.,* **30**: 3770-3775 (2009).

[38] Khadom A.A., Modeling of Corrosion Reaction Data in Inhibited Acid Environment Using Regressions and Artificial Neural Networks, *Korean J. Chem. Eng.*, **30**, 2197-2204 (2013).